Reproductive System in the Male Phase of a Parasitic Isopod (Crustacea) – Morphological, Histological and Ultrastructural Evidence for Sequential Protandrous Hermaphroditic Changes

Article *in* Zoological Studies · October 2019

DOI: 10.6620/ZS.2019.58-04

CITATIONS
4

READS
191

3 authors:

Helna A. K
Kannur University
56 PUBLICATIONS **240** CITATIONS
SEE PROFILE

Sudha Kappalli
Central University of Kerala
57 PUBLICATIONS **510** CITATIONS
SEE PROFILE

Benny K.K. Chan
Academia Sinica
310 PUBLICATIONS **3,414** CITATIONS
SEE PROFILE

Zoological Studies **58:** 4 (2019)
doi:10.6620/ZS.2019.58-04

Zoological Studies

Open Access

Reproductive System in the Male Phase of a Parasitic Isopod (Crustacea) – Morphological, Histological and Ultrastructural Evidence for Sequential Protandrous Hermaphroditic Changes

Helna Ameri Kottarathil[1] and Sudha Kappalli[2,*]

[1]*Post Graduate Department of Zoology and Research Centre, Sree Narayana College, Kannur 670 007, India.*
E-mail: ksudha50@rediffmail.com
[2]*Department of Animal Science, School of Biological Sciences, Central University of Kerala, Kasaragod, Kerala, India.*
**Correspondence: E-mail: sudhakappalli@cukerala.ac.in*

Received 5 October 2018 / Accepted 28 February 2019 / Published 27 March 2019
Communicated by Benny K.K. Chan

This paper reports the protandric hermaphroditic changes in the reproductive system of the male-phased *Norileca indica*, a cymothoid that parasitizes the scombrid fish *Rastrelliger kanagurta*. Each part of *N. indica*'s paired reproductive system lies on either side of the gut. This study considers the three successive size classes of the male phase – designated as M1, M2 and M3 – using light microscopy and ultrastructural methods. The testis comprises of three bulged sac-like lobes labelled t_1, t_2 and t_3, all of which open into the ovary of their respective side. The vas deferens, which emerges as a posterior extension of the ovary, opens into the penis and the distal end of each oviduct leads to a sealed gonopore on their respective sides. Each testis lobe (t_1/t_2/t_3) displays clusters of germ cells undergoing stage-specific differentiation. Spermatids undergoing sequential changes associated with spermiogenesis keep close proximity to somatic accessory cells. The characteristic histological changes associated with protandric hermaphroditism are visible in the ovaries of sequential size classes (M1, M2 and M3). In early M1, besides spermatophores, the ovary has abundant polymorphic nuclei; in the mid/late M1, the posterior ovary has abundant spermatophores, anterior displayed oogonia, previtellogenic oocytes and two distinct forms of follicle cells. In M2, the anterior ovary shows compactly arranged oocytes while the posterior region accommodates spermatophores – fewer, however, than during M1. The entire ovary during M3 is crowded with previtellogenic oocytes, which marginalize the spermatophore passage. The vas deferens of the smallest M1 lack spermatophores. As the size class progresses through late M1 into M2 and M3, the posterior vas deferens is filled with spermatophores, which closely associate with the glandular epithelial lining.

Key words: *Norelica indica*, Protandric hermaphroditism, Male reproductive system, Testis, Ovary, Spermatogenesis, Spermiogenesis.

BACKGROUND

Cymothoids, the parasitic isopod crustaceans, are known to be obligatory parasites of fishes from diverse ecosystems and cause deleterious impacts on them (Trilles et al. 2011 2012; Elshahawy and

Citation: Kottarathil HA, Kappalli S. 2019. Reproductive system in the male phase of a parasitic isopod (Crustacea) – morphological, histological and ultrastructural evidence for sequential protandrous hermaphroditic changes Zool Stud **58:**04. doi:10.6620/ZS.2019.58-04.

Desouky 2012; Hadfield et al. 2013; Aneesh et al. 2013 2014 2015a b 2018). They have also been well recognized as protandrous hermaphrodites, spending the first part of their adult life as males and the later part as females with profuse breeding (Cressey 1983; Brook et al. 1994; Subramoniam 2013, 2016; Ghiselin 1969; Cook 2012). Morphological evidence of protandrous hermaphroditism has been reported in a few cymothoids infesting teleost fishes (Legrand 1952; Juchault 1965; Tsai et al. 1999). The female members of *Ichthyoxenus fushanensis*, a flesh burrowing cymothoid, have a vestigial penis signifying that the species is protandrous hermaphrodite (Tsai et al. 1999). In *Cymothoa oestroides*, *Nerocila maculata*, *N. bivittata*, *Anilocra physodes*, *A. mediterranea* and *Mothocya renardi*, the gonad appears with the ovary and testis, along with their ducts (Bullar 1876; Aneesh 2014). Despite these sporadic reports, information on the hermaphroditic reproductive system in parasitic isopods and its pattern of functioning are still lacking. *Norileca indica*, a cymothoid that profusely infects the Indian mackerel *Rastrelliger kanagurta*, displays characteristic morphological features associated with sequential protandrous hermaphroditism from the juvenile to the adult phase; these comprise three successive phases such as male, transitional and female (Helna 2016). While this cymothoid (*N. Indica*) is in its male phase, no female morphological characters are expressed. An interesting question about *N. indica* is if the reproductive system in the male phase is devoted exclusively to the production of male gametes, or if the gonad simultaneously begins to prepare for the female gametes. This paper demonstrates for the first time the sequential protandrous hermaphroditic changes in *N. indica*'s reproductive system during its male phase. The reproductive system of three sequential and morphologically distinct size classes during the male phase—designated M1, M2 and M3—were considered for the present light microscopic and ultrastructural studies. An attempt was also made to gather data on spermatogenesis, spermiogenesis, sperm discharge and the structure of spermatozoa in the candidate species.

MATERIALS AND METHODS

Collecting *Norileca indica*

Norileca indica was collected from the branchial cavity of its host fish, *Rastrelliger kanagurta*, obtained from the Ayikkara Fish Landing Centre (11°51'33"N, 75°22'30"E; Malabar Coast, India) from July 2011-July 2015. Additional collections were made from March 2017-May 2018. Three sequential and morphologically distinct size classes (M1, M2, M3) of the *N. indica* adult male phase were categorized using body length and width as criteria. M1 (early size male formed right from the juvenile through molting) has 9.0-12.9 mm long and 3.5-4.5 mm wide. The size of M2 ranges from 13.0-17.9 mm in length and maximum 7.0 mm in width and that of M3 is 18.0-20.0 mm in length and maximum 12.0 mm in width.

Morphological study of reproductive systems and gametes

The hermaphroditic reproductive system from all size classes (M1, M2 and M3) of male *N. indica* was dissected out by cutting open the terga in 0.9% saline solution under a stereo dissection microscope (Leica-S6D) and their stage-specific morphological features were observed. Gonad size was measured and visible cells counted using micrometry. The gonad was incised using a fine needle and the spermatozoa that oozed out were observed under a Leica microscope (DM 750).

Histology and histochemistry of the reproductive system

Ovary, testis and their respective ducts were separated from the formol-alcohol fixed hermaphroditic reproductive system derived from M1, M2 and M3. The tissues were paraffin wax embedded, sectioned (3-4 µm thickness) and double stained with Harri's haematoxylin and 1% alocoholic eosin (Humason 1967). For the purpose of light microscopic observation, semi-thin sections (1.0 µm) of Karnovisky-fixed (4% paraformaldehyde and 3% glutaraldehyde at pH 7.2) gonads (ovary and testis) were also stained with methylene blue. The histochemistry was done using Mercuric Bromophenol Blue (proteins), PAS (carbohydrates), Sudan Black (lipids) and Basic Fuchsin (DNA) (Pearse 1968).

Electron microscopy

The hermaphroditic reproductive system from M1, M2 and M3 was fixed in Karnovsky's fixative for 24 hours and processed according to the procedure described by Williams and Carter (1996). Briefly, the fixed tissue was washed with phosphate buffer (pH 7.4) for approximately 15 minutes and post-fixed in 1% osmium tetroxide (OsO_4). After further washing with phosphate buffer for half an hour, the tissue was dehydrated in ethanol grades followed by en bloc staining (2% uranyl acetate in 95% ethyl alcohol) and dehydration. Clearing and embedding were carried out in propylene oxide and araldite, respectively. Ultrathin

sections (grey to silver) stained with uranyl acetate and lead citrate were examined under a Transmission Electron Microscope (Tecnai G2) in the facility extended from the National Institute of Mental Health and Neurosciences (NIMHANS), Bangalore.

Documentation

Photomicrography was done using a Leica ICC50 camera (attached to a Leica research microscope -DM-750) and Canon Power Shot S 50 camera (attached to a Leica Stereo Zoom -S6 D) and microscopic image capturing and processing software (LAS EZ, Leica Application Suit-Version 1.7.0).

RESULTS

Morphology of hermaphroditic reproductive system in male-phased *N. indica*

In male-phased *N. indica* (Fig. 1A), the paired hermaphroditic reproductive system lies one on either side of the gut below the nerve tract and extends between the 4th and 6th pereonites. Both the ovary and testis on each side form a continuous structure in which the ovary appears simple and elongated while the testis comprises three bulged sac-like lobes labelled t_1, t_2 and t_3, located on the antero-lateral side of the ovary (Fig. 1B). The vas deferens emerges as a posterior extension of the ovary and opens into the penis located

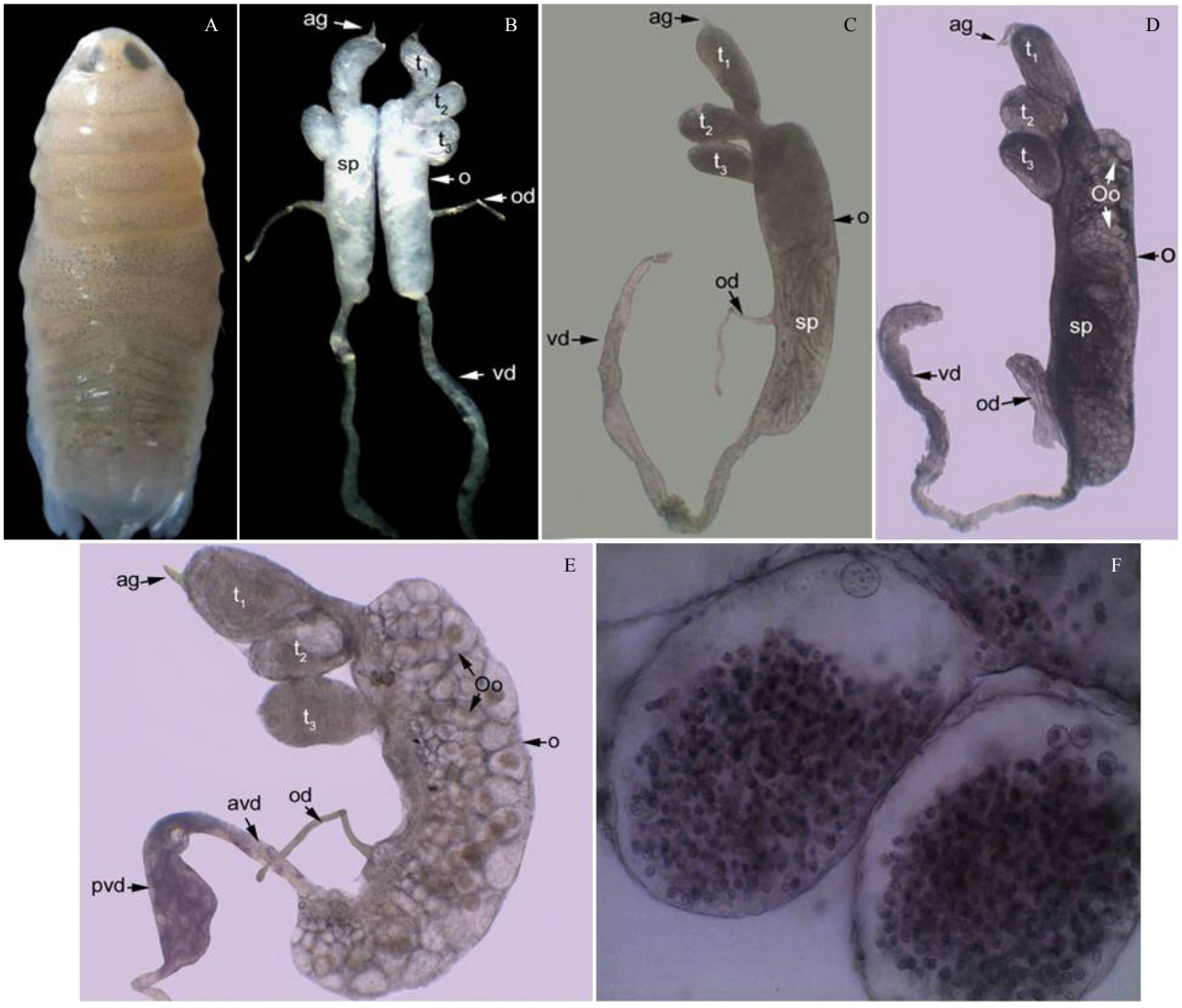

Fig. 1. *Norileca indica* and its protandrous hermaphroditic reproductive system. A. *Norileca indica* – male; B. paired structure of gonad (20 X); C-E. Gonad in different male stages (C: M1, D: M2, E: M3) (40 X); F. testes lobes showing different staged cells and germarium. t_1, t_2, t_3- testis lobes 1-3, o- ovary, od- oviduct, vd- vas deferens, avd- anterior vas deferens, pvd- posterior vas deferens, Oo- oocytes, sp- spermatophore, ag- androgenic gland.

at the sternite 7. The slender and inconspicuous tubule-like oviduct (Figs. 1 B-E) extends laterally from the mid ovary and ends in the sealed gonopore located at the 6th pereonite (Fig. 1D); the average length of the reproductive system found in M1, M2 and M3 is 1.38 mm, 1.39 mm, and 1.40 mm, respectively (Table 1).

Testis

Testis was significantly different between M1, M2 and M3 (Table 1). Irrespective of size class, all the three testis lobes (t_1, t_2 and t_3) were bulged and t_1 was relatively large in size compared to t_2 and t_3 (Table 1). All three lobes tapered posteriorly and while t_1 and t_2 were close to each other, sharing a common duct leading to the antero-lateral side of the ovary; t_3 was slightly isolated from the duo, and light microscopic observations showed it had a separate duct (Figs. 1C; 2A). The androgenic gland was seen attached to the antero-lateral side of t_1 (Fig. 1D, E).

Germ cells undergoing different stages of differentiation were clearly visible while viewing the gonad under the light microscope (Fig. 1F). The testis in M1 had abundant primary and secondary spermatogonia (Fig. 2B) and, in the successive stage (M2), spermatocytes—as well as spermatogonia—were also visible at different meiotic stages (Figs. 2C, D). In M3, the testis had abundant spermatogonia, spermatocytes, spermatids, spermatozoa and spermatophores (Fig. 2E).

Both primary and secondary spermatogonia usually occupy the periphery of the testis, irrespective of the lobe (t_1, t_2 and t_3). In our close observation, it is also evident that each testis lobe displays clusters of germ cells undergoing specific stage of differentiation; for instance, in t_1, while one half portion is abundant with spermatozoa/spermatophores, the other half houses the germ cells undergoing spermatogenesis, of which meiotically dividing spermatocytes are dominant (Fig. 3A). Most of the spermatophores were found to be closely associated with somatic accessory cells (Fig. 3B). The histological section of t_2 (of the same testis) shows the presence of spermatogonia as well as spermatocytes, whereas t_3 not only has abundant spermatogonia and spermatocytes but also spermatids (Figs. 3C, D). The spermatids (in t_3) were also seen at different stages of spermiogenesis (Fig. 3D). Histochemically, the testis lobes of M1, M2 and M3 tested positively for carbohydrate, protein and lipid (Fig. 4).

Germ cells undergoing differentiation: Light and Electron microscopic view

The primary spermatogonia (7.0-11.0 µm) possessed a relatively large nucleus with nucleolus- and peripherally-distributed chromatin; in the nucleus of secondary spermatogonia (5.0-9.0 µm), the chromatin was found to be more or less scattered (Fig. 2B). Under the light microscope, both primary and secondary spermatocytes (size 6.90 ± 0.42 µm) were characterized by the presence of highly condensed chromatin, and many of them were found with meiotic stages (Figs. 2C, D). Ultrastructurally, spermatocytes were rich in mitochondria and membrane-bound vesicles (Fig. 5A). Relatively small (3.79 ± 0.39 µm) spermatids with centrally placed spherical nuclei along with its nucleoli were distinct (Figs. 2E; 3D). In both light and electron microscopic view, many of the spermatids kept close in proximity to the somatic accessory cells and were likely under the process of spermiogenesis. By the onset of spermiogenesis, the nucleus of the newly-formed spermatids conical bulges, apparently for the formation of acrosomal vesicle (Figs. 2E, F), and the heterochromatin condenses and remains close to the nuclear envelope, resulting in the formation of incomplete rings of variable thickness. With the progress of spermiogenesis, the bulged nuclear pole elongates while the opposite pole remains vesicular. The

Table 1. Micrometric measurements of reproductive structures in *N. indica*'s male phase

Male stages	Reproductive structures with size			
	Testis	Ovary	Vas deferens	Oviduct
M1	t_1: 344.704 ± 96.41 µm in length t_2: 244.55 ± 53.86 µm in length t_3: 228.67 ± 42.95 µm in length	791.405 ± 12.92 µm in length	1650 ± 0.95 µm in length, 32.4 ± 2.07 µm in width	272 ± 2.64 µm in length, 19.07 ± 0.69 µm in width
M2	t_1: 352.48 ± 82.96 µm in length t_2: 283.35 ± 106.57 µm in length t_3: 256.012 ± 102.76 µm in length	1800.58 ± 0.62 µm in length	2941.007 ± 59.93 µm in length, 98 ± 0.5 µm in width	277.66 ± 19.39 µm in length, 19.23 ± 0.05 µm in width
M3	t_1: 387 ± 142.14 µm in length t_2: 277.81 ± 219.74 µm in length t_3: 259.85 ± 123.28 µm in length	3407 ± 26.14 µm in length	2680.14 ± 65.32 µm in length, 289.25 ± 120.9 µm in width	275.2 ± 14.23 µm in length, 23.25 ± 0.35 µm in width

gradual elongation of the nuclear pole eventually results in the formation of a ribbon-shaped nucleus with the simultaneous reduction of cytoplasm and subsequent degeneration of the vesicular part (Fig. 2F). Overall transformation culminates in the formation of unique-shaped spermatozoon with ribbon-like nuclear head and apexed acrosome thickly wrapped with extracellular tubules (Figs. 2H; 5C). The cell boundaries gradually disappear and the nuclei are seen in the common cytoplasmic mass; many of these nuclei found clustered

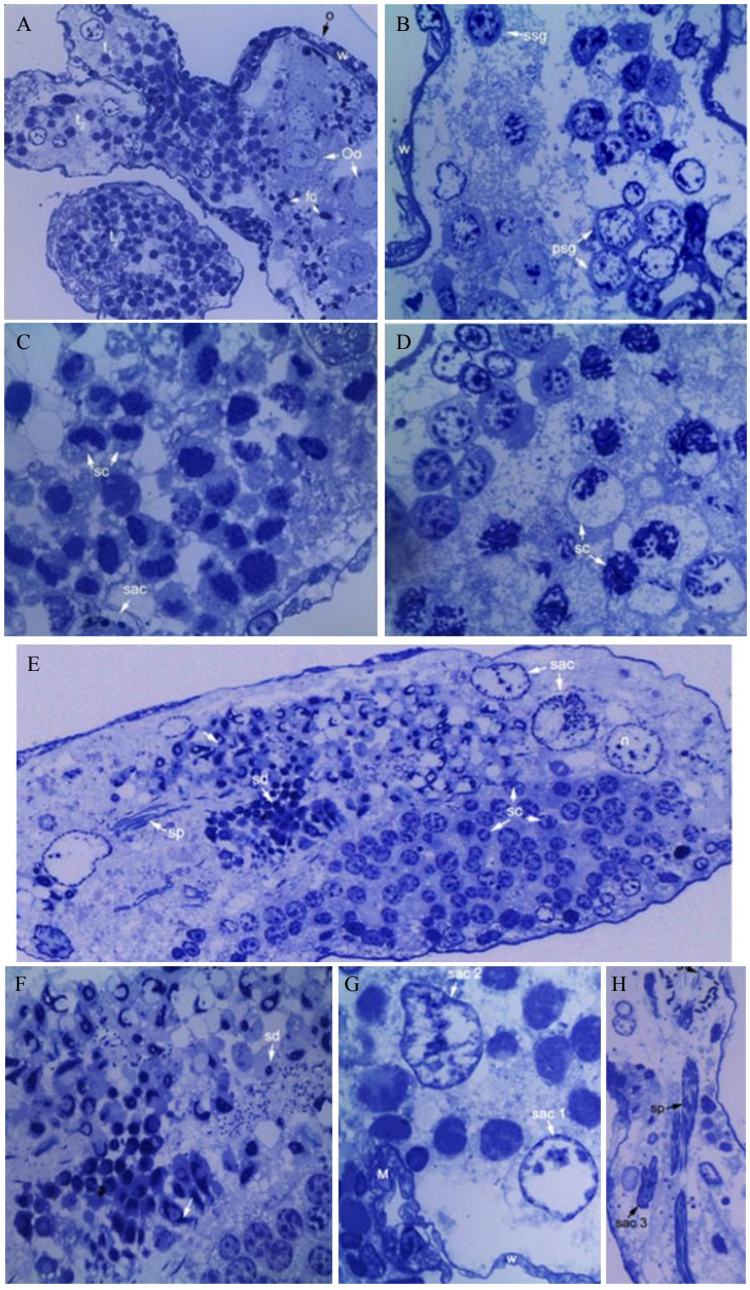

Fig. 2. *Norileca indica* – hermaphroditic gonad in male stages. A. anterior gonad showing the connection between the testis lobes and the ovary (200 X); B. testis (M1) showing spermatogonia (1000 X); C. testis (M2) showing spermatocytes at equatorial plate forming stage of meiosis and somatic accessory cells (1000 X); D. spermatocytes at different meiotic stages (1000 X) (semithin LS: 1 µm; Methylene blue). Testes showing E. regionalization of germ cells undergoing spermatogenesis and spermiogenesis (M3) (200 X); F. spermiogenesis (arrow showing elongation of spermatid nucleus) (1000 X); G. somatic accessory cell types (1000 X); H. somatic accessory cell, spermatophores and spermatozoa (400 X). t_1, t_2, t_3 - testis lobes 1-3, Oo- oocyte, w- wall, psg- primary spermatogonia, ssg- secondary spermatogonia, sc- spermatocyte, sac- somatic accessory cell, o- ovary, fc- follicle cell, sac- somatic accessory cell, sd- spermatid, sc- spermatocyte, n- nucleus, sp- spermatophore, s- spermatozoa, sac 1, sac 2, sac 3 - somatic accessory cell types 1-3, w- wall, M- muscle.

and the cytoplasmic extremities become more elongated to form tails and their further association culminates in the formation of the characteristic sperm bundle designated as spermatophore (Figs. 4A-D).

Spermatophore and spermatozoon: Light and electron microscopic view

In eosin-hematoxylin stained smear preparation, the spermatophore's nuclei were basophilic, while the tails were strongly acidophilic (Fig. 4F). Under the electron microscope, the longitudinal and cross sections of spermatophore tails appeared as a cluster of discs and each disc (representing the cross/oblique section of a sperm tail) showed the presence of a central lumen filled with electron light and dense materials (Figs. 5D, E). Also, the cross sections of spermatophore's nuclei were seen as electron dense discs. The spermatophores, closely associated with the somatic accessory cells were found to be enriched with both RER and mitochondria (Figs. 5F, G). Spermatozoon was characterized by its long, non-motile tail (length 0.90 ± 0.06 mm) and ribbon-like nucleus (0.06 ± 0.01 mm), joined together with an acrosome to form the head. The head projected laterally from the tail at an acute angle, giving the spermatozoon a flag-like appearance, tapering at its distal end (Figs. 4D, E; 5H). The tail expressed a high degree of histochemical affinity to MBB and PAS tests but poor affinity towards Sudan Black. On the other hand, the nucleus was strongly/moderately positive for all the tested histochemical stains (Basic Fuchsin, MBB, Sudan Black and PAS) (Figs. 4G-I). The nuclei of the spermatophore were embedded in a large number of microtubules (Fig. 5C) and the mitochondria were found between the nucleus and the acrosome (Fig. 5G).

Somatic accessory cell: Light and Electron microscopic view

In the testes of *N. indica*, a somatic accessory cell (sac) appears to be large, with an irregular and polymorphic nucleus and its three forms were identified and labelled sac 1, sac 2 and sac 3 (Figs. 2G, H). Sac 1 occupied the periphery of the testes and possessed an oval/spherical basophilic nucleus 16.5 ± 2.10 µm large; under the electron microscope, the nucleoplasm

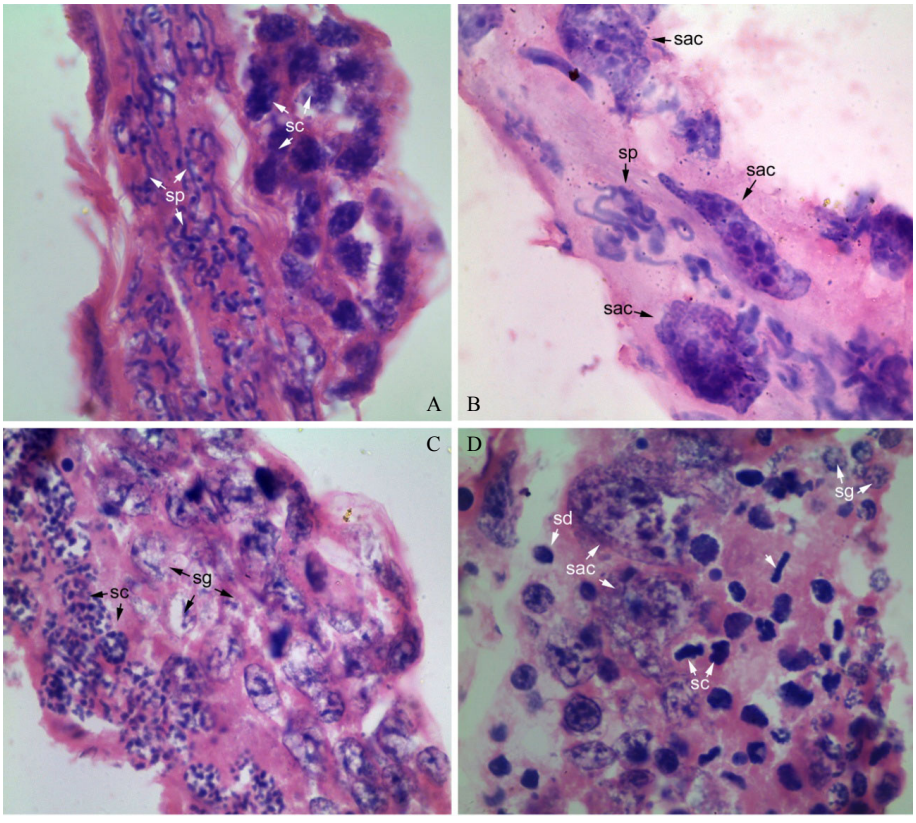

Fig. 3. Histological section of testicular lobes (t_1, t_2, t_3) of male *N. indica* (LS: 3 µm, Haematoxylin-Eosin) depicting asynchrony in spermatogenesis (1000 X) A. t_1 showing spermatocytes and spermatophores; B. t_1 showing the association between spermatophores and somatic accessory cells; C. t_2 showing spermatocytes at pachytene stage and spermatogonia; D. t_3 showing spermatocytes at equatorial plate forming stage of meiosis (arrow), spermatid and somatic accessory cells. sp - spermatophore, sc- spermatocytes, sac- somatic accessory cells, sg- spermatogonia, sd- spermatid.

was enriched with electron-dense heterochromatin that adhered to the membrane (Figs. 5B, F). The nucleus of sac 2 possessed a distinct nucleolus 9.14 ± 1.48 µm in size (Fig. 2G). sac 3 appeared to have a more elongated spindle-shaped nucleus 14.21 ± 0.98 µm large and its pattern of chromatin condensation was different from the former ones (Fig. 2H).

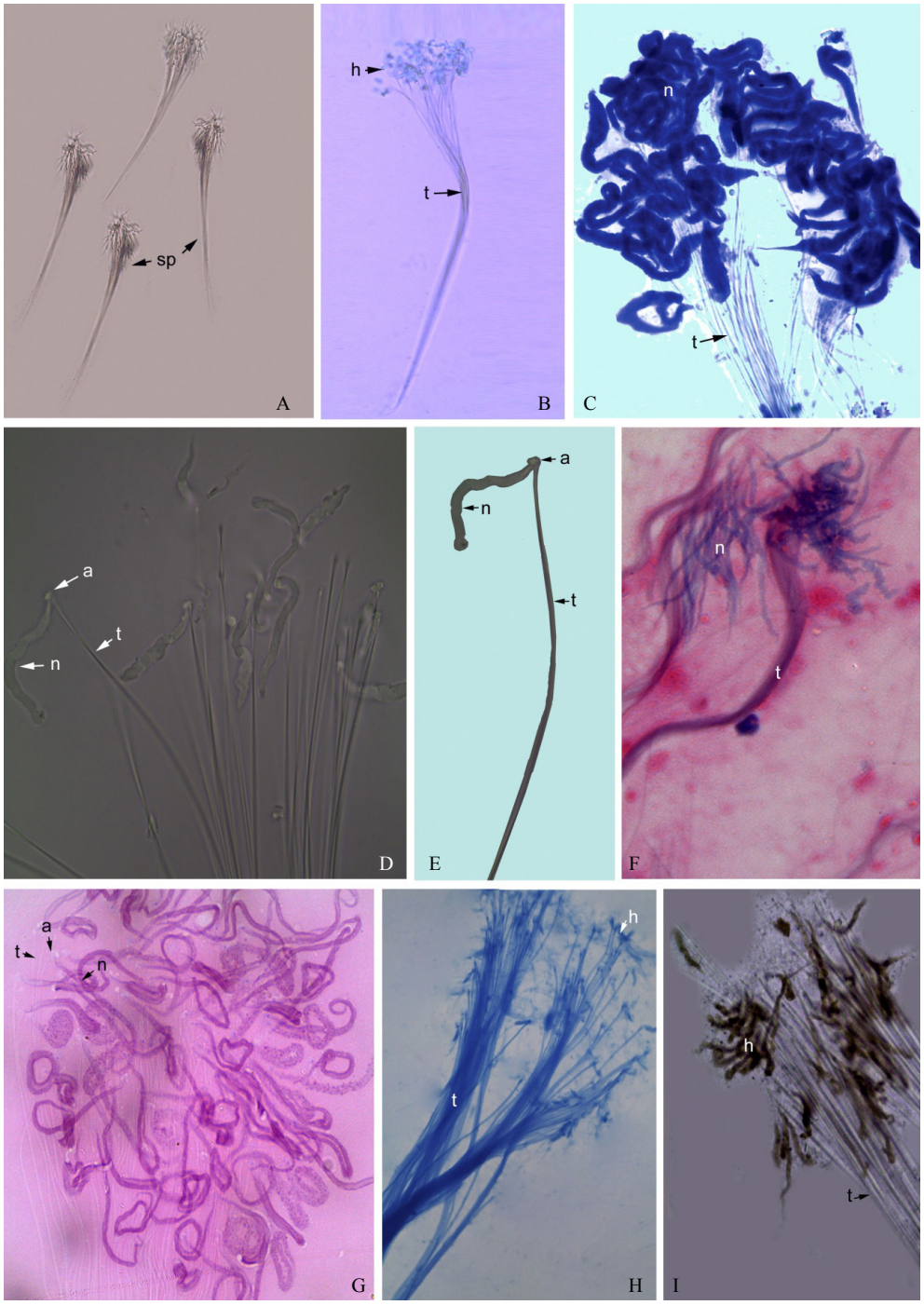

Fig. 4. *N. indica* male A. spermatophores (unstained) (100 X); B. methylene blue stained single spermatophore (200 X); C. spermatophore heads showing positivity to methylene blue (1000 X); D. spermatophore (unstained) (1000 X); E. spermatozoon showing distinct nucleus, acrosome and tail (1000 X); F. spermatophores (Haematoxylin-Eosin) (400 X); G. spermatophore heads showing positivity to basic fuchsin (1000 X); H. spermatophore showing positivity to bromophenol blue (1000 X); I. spermatophore heads showing positivity to Sudan Black (1000 X). sp- spermatophore, t- tail, a- acrosome, n- nucleus, h- head.

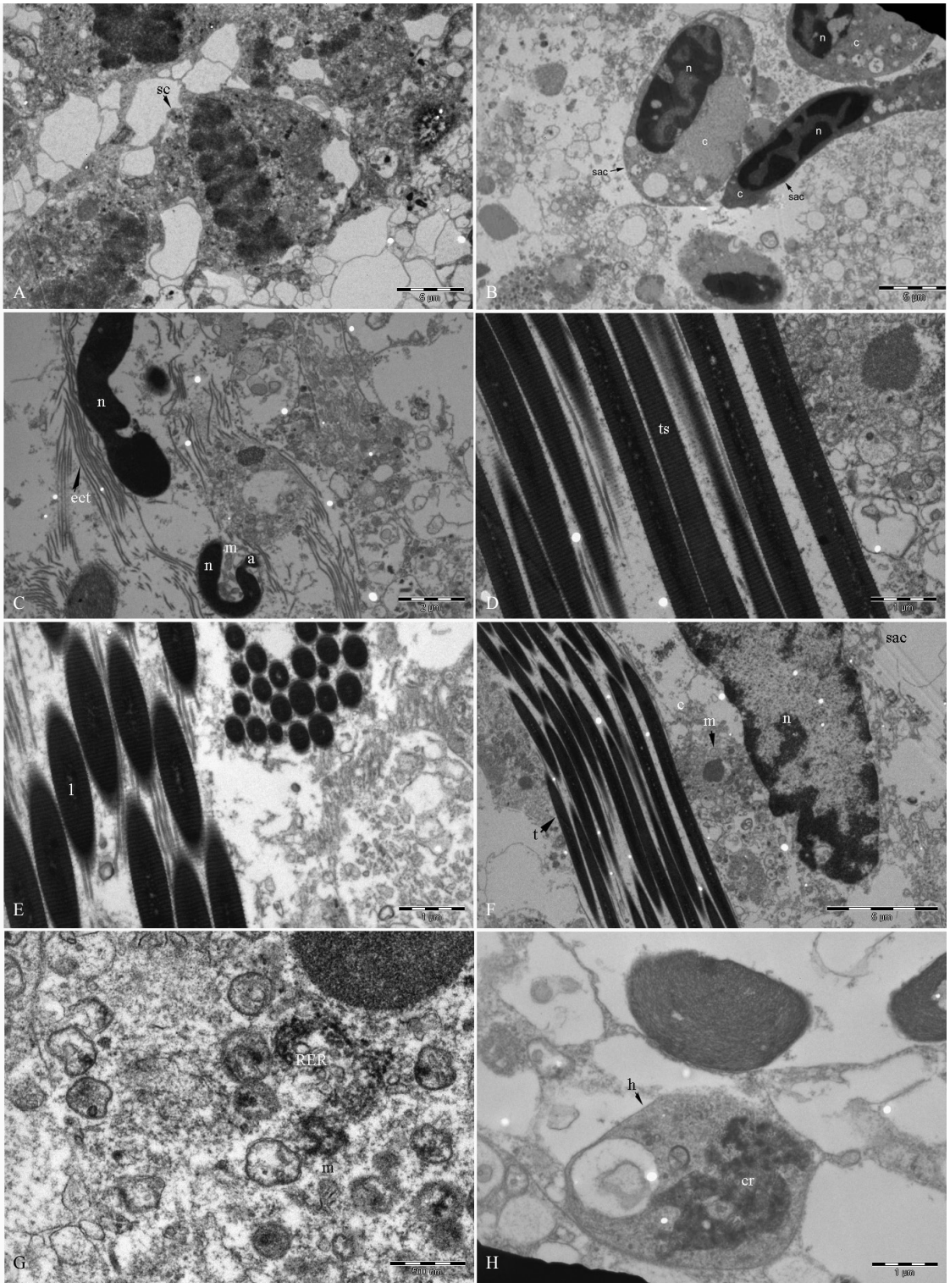

Fig. 5. Electron micrographs of testis in male stage of *N. indica* showing A. spermatocyte (arrow) at meiotic stage (equatorial plate formation) (2900 X), B. somatic accessory cells (2900 X), C extracellular tubules and nuclei of spermatozoa (6800 X), D. tails of spermatozoa showing striations and central lumen (13000 X), E. clustered spermatophore tails (13000 X), F. spermatophore associated with somatic accessory cells (4800 X), G. somatic accessory cell cytoplasm showing cell organelles (30000 X), H. head of spermatozoon (13000 X). sac- somatic accessory cell, sc- spermatocyte, c- somatic accessory cell cytoplasm, n- somatic accessory cell nucleus, n- somatic accessory cell nucleus, t- spermatophore tail, ts- transverse striations, m- mitochondria, RER- Rough endoplasmic reticulum, *l*- lumen, n- nucleus, *l*- lumen, h- head, cr- chromatin, ect- extracellular tubules, a- acrosome.

Ovary

M1: Ovary (average length - 568.0 µm) of the prestaged M1 (size - 8.8 mm) showed the presence of cells with large vacuoles and deeply stained peripheral nuclei (Fig. 6A). In M1 (size 9.0 mm), the ovary (size 1.05 ± 0.21 mm) had abundant oogonial cells and spermatophores (Fig. 7B). The histological sections displayed a large number of randomly distributed polymorphic nuclei (size 4.7 - 7.5 µm) with condensed chromatin, which are apparently the precursors of the prospective oocytes or follicle cells (Figs. 6B; 7A). Our histological observations concluded that the epithelial wall of the ovarian lobe is secretory (Fig. 7G). During the mid and late stages of M1, spermatophores were found aggregated at the posterior ovary, orienting their heads invariably toward the mouth of the vas deferens (Fig. 7E). Meanwhile, the anterior ovary had abundant previtellogenic oocytes (size 276.02 ± 44.53 µm) with large nuclei (size 135.82 ± 18.71 µm) and nucleoli.

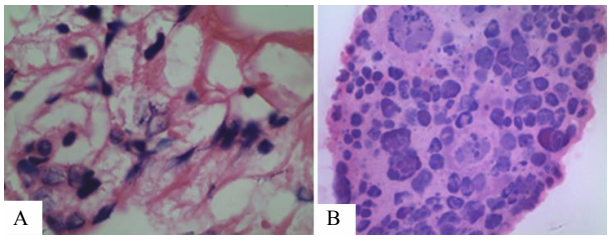

Fig. 6. Histology of ovary in male stages (M1, M2, M3). A. prestaged M1 ovary B. M1 ovary.

Antero-laterally, the ovary was occupied by high prolific germarium and differentiating/differentiated oogonial cells (Fig. 1E). Some of these cells (size 121.56 ± 10.66 µm) possessed a large nuclei (size 82.48 ± 9.30 µm) and the cytoplasm—filled with vesicles containing dense basophilic granules—were displaced towards the posterior ovary (Fig. 7C).

Two forms of follicle cells (labelled fc1 and fc2) with size ratio 2:1 were found to be associated with the oocytes; fc1 (size 6.94 ± 1.07 µm) appeared with a highly basophilic round/oval nucleus (size 5.9 ± 0.26 µm) and a rim of cytoplasm; the nucleus of most fc1 cells also had relatively large condensed chromatin granules and nucleolus (Fig. 7F). The relatively elongated fc2 cells displayed a distinct nucleus (8.9 µm) and highly condensed chromatin, but no distinct nucleolus (Figs. 7B, F). Ultrastructurally, the cytoplasm of both fc1 and fc2 were enriched with RER, golgi, free ribosomes, mitochondria and secretory vesicles and some of the vesicles were found fused with the plasma membrane (Figs. 8C-E). Two subpopulations of fc1 were also recognized; one with a rim of cytoplasm and a large, oval nucleus showing diffused electron lucent euchromatin and peripheral electron-dense heterochromatin; the other with spherical large nucleus had thread-like heterochromatin and a high proportion of euchromatin (Fig. 8A).

M2: The ovary in M2 attained a length of 1.86 ± 0.62 mm and accommodated a large number of yolkless (previtellogenic) oocytes (size 121.56 ± 10.66 µm) with a distinct nucleus (size 82.48 ± 9.30 µm) and a

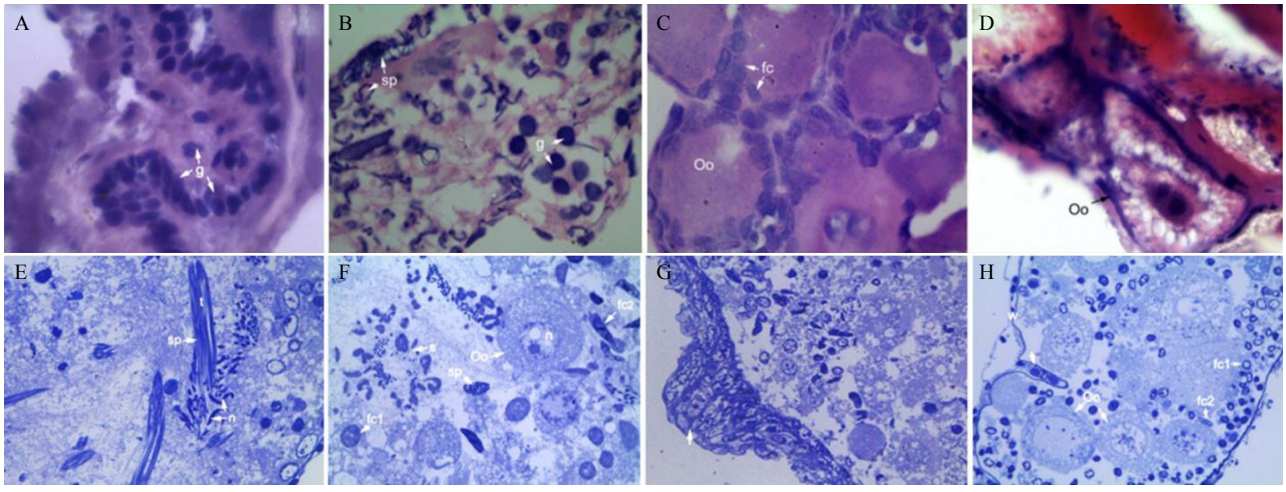

Fig. 7. Histological and histochemical observation of ovarian germ cells and oocytes (*N. indica*) during male phase of *N. indica*. (LS: 4 µm; Haematoxylin-Eosin; 1000 X) A. germ cells (in M1); B. spermatophore and germ cells (in M1); C. follicle cells enveloping the oocytes (in M2); D. oocytes (in late M3); semithin LS: 1 µm; methylene blue showing E. spermatophores (M1) (400 X); F. follicle cells, previtellogenic oocytes and spermatophores (M2 1000 X); G. bulged ovarian wall (arrow) (400 X); H. ovarian wall showing involution (M2) (arrow) (400 X). g- germ cells, sp- spermatophore, Oo- oocytes, fc- follicle cells. sp- spermatophore, t- tail, Oo- oocytes, fc1- follicle cell type 1, fc2- follicle cell type 2, n- nucleus, s- sperm, w- wall.

rim of cytoplasm (Figs. 7C, H); the average nucleo-cytoplasmic ratio was 2.71. No uniformity was found in the distribution of these previtellogenic oocytes; in the anterior region of the ovary, they were compactly arranged, but in the mid and posterior region, they were found scattered (Figs. 1C; 7H). Contrary to those found in M1, the follicle cells of M2 did not show any distinct cellular boundaries. Nevertheless, their nuclei contained condensed chromatin granules and appeared basophilic, signifying that they are secretory (Fig. 7H). Two distinct types of follicle cells were identified according to their nuclear size and shape: 1) round cells 5.85 ± 0.52 µm

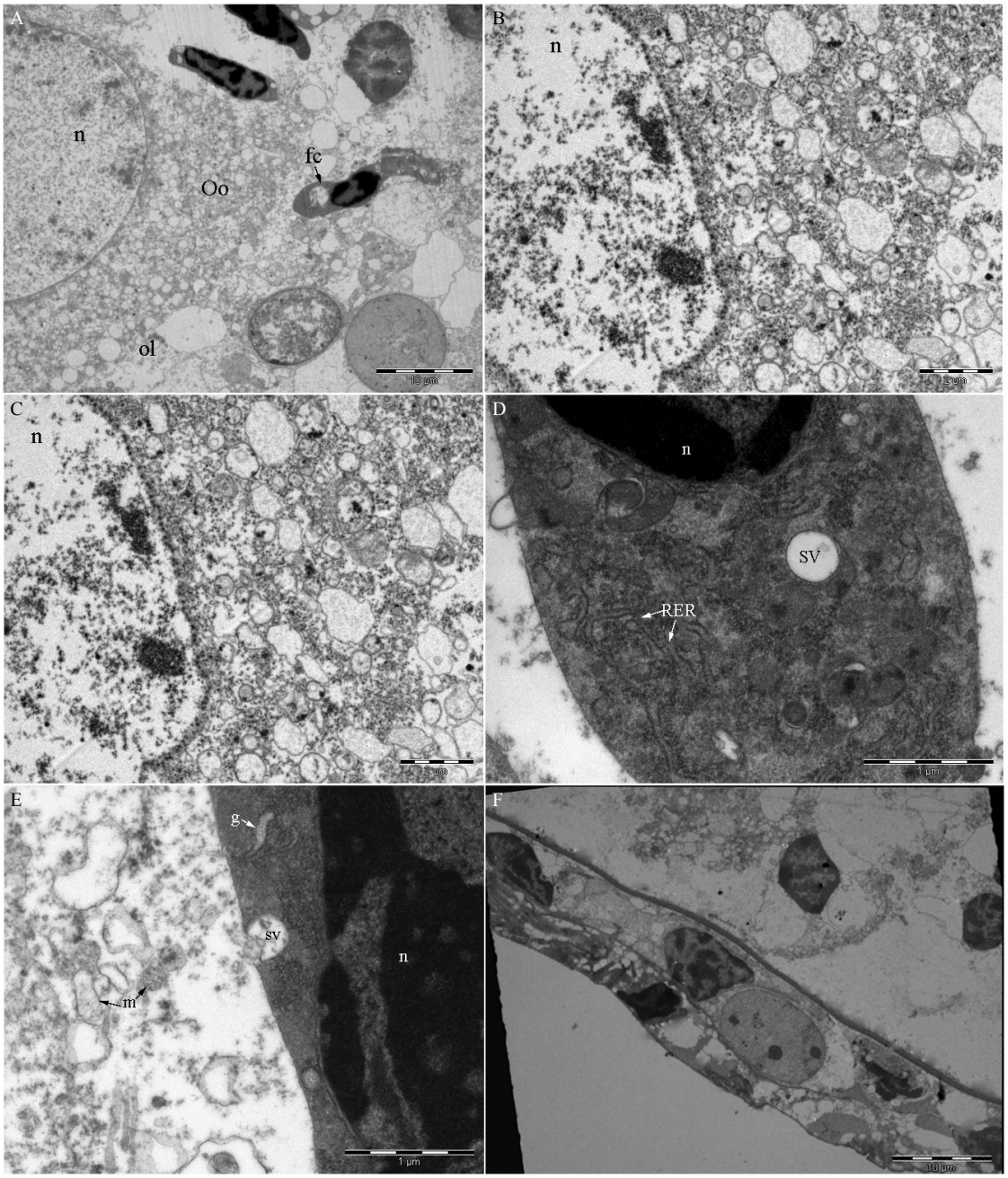

Fig. 8. Electron micrographs of ovary during male stages of *N. indica* A. previtellogenic oocytes associated with follicle cells (1900 X); B. previtellogenic oocytes showing ribosome associated nuclear membrane (6800 X); C. different types of follicle cells (1900 X); D. follicle cell cytoplasm showing RER and protruded plasma membrane (arrow) (23000 X); E. follicle cell cytoplasmic vesicle fused with the plasma membrane (23000 X); F. Wall of the ovary at male stage. Oo- oocytes, fc- follicle cell, n- nucleus, n*l*- nucleolus, r- ribosomes, m- mitochondria, nm- nuclear membrane, o*l*- oolemma fc1- follicle cell type 1, fc2- follicle cell type 2, n- follicle cell nucleus, c- follicle cell cytoplasm, sv- secretory vesicle, g- golgi.

large and 2) elongated cells 8.02 ± 0.55 μm large.

Contrary to the observation in M1, the spermatophores in the M2 ovary got sidelined along the ovarian length right from the neck of t1, apparently due to the invasion of the oocytes (Fig. 1E).

M3: The ovary in M3 attained a length and width of 3.41 ± 0.57 mm and 0.42 ± 0.03 mm, respectively, and was entirely occupied by the previtellogenic oocytes with distinct nuclei and one or two nucleoli (Figs. 1E; 7D); the postero-lateral region of the ovary had abundant small oocytes, whereas the anterior region displayed relatively large oocytes with follicular envelope (Fig. 1E). Ultrastructurally, the cytoplasm of the previtellogenic oocytes had abundant mitochondria, RER, ribosomes (free in the cytoplasm or adhered to the nuclear membrane) and secretory vesicles. In some cases, the nucleus appeared with double nucleoli (Figs. 8A, B). The lumen of the secretory vesicle was filled with either electron dense or lucent bodies (Figs. 8D, E). The nucleus contained euchromatin and scattered or condensed heterochromatin; the nucleolus was peripheral and electron dense (Fig. 8A). In addition, these previtellogenic oocytes were strongly positive for histochemical stains such as MBB, PAS and Sudan Black.

In early M3, the spermatophores in the ovary got intensely marginalized along the ovarian length. Subsequently, in the mid and late M3, no spermatophores were noticed in the ovary (size 19.5-20.0 mm).

In all size classes (M1, M2 and M3) of the male phase, the ovarian wall appeared to be thick and muscular with distinct irregular folding; the epithelial lining displayed polymorphic nuclei (3.5-6.0 μm) that were found aggregated in a random manner (Figs. 7G; 8A). Two forms of the nucleolus in the epithelial cells were found under the electron microscope: one appeared oval with high heterochromatin content and the other was elongated with moderate heterochromatin content (Figs. 8A, F).

Vas deferens (VD)

The thin tubule-like VD (length and width were 1.65 ± 0.10 mm and 0.03 ± 0.002 mm, respectively) in the smallest M1 (9.00 mm) contained no spermatophores, whereas in the late staged M1 (12.00 mm), the posteriorly bulged VD was found to be packed with spermatophores. Throughout the length of the VD, the epithelial wall was festoon shaped (Fig. 1C).

The VD length in M2 and M3 was 2.94 ± 0.06 mm and 2.68 ± 0.07 long, mm respectively (Fig. 1D), and the bulged posterior half of the VD in both size classes indicate the presence of spermatophores (Figs. 1D-E); the average diameter of the anterior, mid and posterior part of the VD in M3 was 0.12 μm, 0.21 μm and 0.40 μm, respectively.

In both semi-thin and ultrathin sections, concentric layered blocks of fibrous tissue were visible along one side of the VD wall in M2 (Figs. 9D-E). The opposite side, however, displayed only the glandular epithelial lining, the cells of which possess a distinct basophilic nucleus with nucleolus. Two epithelial cell types were identified based on the size and shape of the nucleus, one with a more or less round nucleus (size 9.09 ± 1.23 μm) and the other with an elongated one (size 13.11 ± 3.16 μm) (Figs. 9D-E); the nuclei appeared electron dense and the cytoplasm contained RER.

Irrespective of size class (M1, M2 and M3) of the male phase, the lumen of the VD had acidophilic substances that are likely secretion from the epithelium. The lumen of the mid and posterior VD in M2 and M3 had abundant spermatophores that were embedded in the secretory substance (Figs. 9A-C). Interestingly, in most instances, the clubbed tails of the spermatophore were closely associated with the epithelial cells (Fig. 9C). The entire contents of the VD were strongly positive to histochemical tests such as MBB, PAS and Sudan Black.

Oviduct

The length and width of the oviduct was 275.8 ± 14.00 μm and 19.07 ± 0.69 μm, respectively, in the early staged M1 and the width showed a marked increase (23.25 ± 0.35 μm) in the late staged M3 (Figs. 1A-D). Also, a thin layered epithelial wall was observed with relatively small basophilic nuclei (Fig. 9F).

DISCUSSION

In the light of the results tracking the reproductive system of the three size classes of the male-phased *N. indica*, at morphological and cytological levels, it is evident that this parasitic isopod exhibits a strict sequential protandrous hermaphroditic mode of reproduction. In the *N. indica* larval form (manca II), gonad primordia appeared as a simple tubule while in the juvenile form, the reproductive system consisted of three testicular lobes and a simple tubular ovary with respective ducts; the cells in the testis lobes and ovary were homogenous in appearance (Helna 2016). Though both testis and ovary appeared as distinct structures from early in M1, results from this study suggest that spermatogenesis likely precedes oogenesis. The testes were functionally active in all the three male size classes

(M1, M2 and M3). The progressive changes in the ovary associated with oogenesis begin in M2, judging by the presence of previtellogenic oocytes. It is significant to note that, despite their inertness, none of the components or structures in the male hermaphrodictic reproductive system of *N. indica* showed signs of complete degeneration. The sequential protandrous hermaphroditic changes during the male phase were clearly depicted in *N. indica*: 1) In the prestage M1, the presence of some spermatophores in the testis indicates the organ is functional. Meanwhile, there were no oocytes in the ovary and no spermatophores in the vas deferens. 2) In M1, apart from the testis, an enormous number of spermatophores were found in the vas deferens and entire ovary, but only a few oocytes were found in the ovary. 3) In M2, the testis was actively undergoing spermatogenesis and spermiogenesis. Spermatophores were mostly limited to the posterior part of the ovary. The spermatophores' passage from the ovary into the vas deferens was marginalised due to the largenumber of enlarging oocytes, and the entire vas deferens bulged due to the presence of enormous spermatophores. 4) In M3, the testis underwent spermatogenesis and spermiogenesis, spermatophores became more marginalized in the ovary due to thickly and compactly filled oocytes. The region of the vas deferens close to the genital aperture bulged because it was filled with spermatophores. 5) *Norileca indica* was about to moult in M3, and only a few spermatophores were seen in the testis; the ovary was completely filled with oocytes, showing the sign of yolk deposition; and few spermatophores were found in the vas deferens.

Protandrous hermaphroditism is uncommon, but it has been reported in free living and parasitic non-isopod crustaceans. In the thalassinid *Calocarinus macandreae*, the testis and ovary grow at an approximately equal rate until the testis reaches its maximum size. Then the testis degenerates and the ovary continues to increase in size, completely filling the space of the degenerated testis; in the meantime, the vas deferens is retained throughout its life, filled with spermatophores (Buchman 1963). In the shrimp *Pandalus borealis*, Allen (1959) observed that oocytes are present in the central region of the gonad tract during the male phase. Bilaterally asymmetrical hermaphroditism is also found in lobsters such as *Nephrops norvegicus* and *Homarus* sp., in which the internal and external male characteristics are found on one side of the body and female characteristics on the

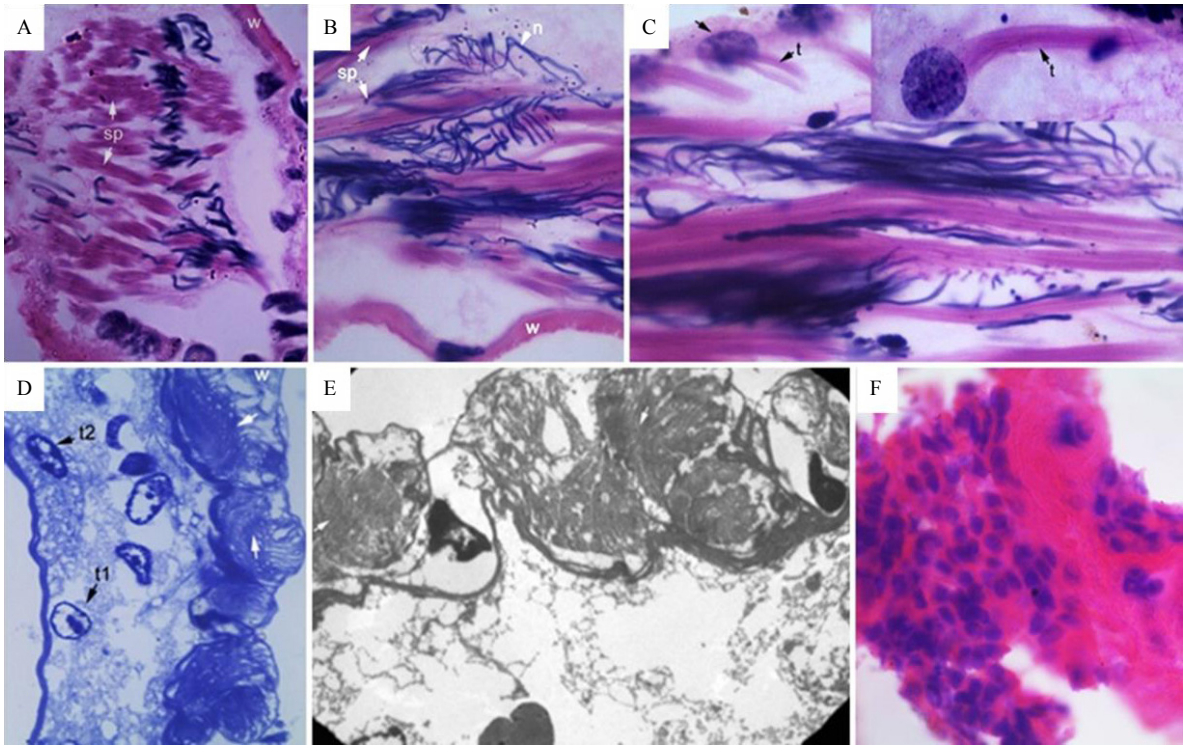

Fig. 9. Vas deferens of male staged *N. indica* showing A. spermatophores and secretory epithelial wall (CS: 3 µm; Haematoxylin-Eosin) (1000 X), B. spermatophores (LS: 3 µm; Haematoxylin-Eosin) (400 X), C. association of spermatophore tails with the secretory epithelial layer (1000 X) (inset-enlarged view); semithin section D. (1000 X) and electron micrograph E. showing concentric layered fibrous tissue associated with the wall of the vas deferens (arrow) (1400 X). F. Oviduct. sp- spermatophore, t- tail, Oo- oocytes, t1- type 1 epithelial cell, t2- type 2 epithelial cell, n- epithelial cell nucleus, w- epithelial wall.

opposite side (Schram et al. 2012). In hermaphroditic species of caridean shrimps and crayfishes, the anterior and posterior parts of the gonad correspond to the ovary and the testis, respectively (Bauer and Holt 1998).

In general, the protandrous hermaphroditic gonad in *N. indica* morphologically resembles that of other cymothoids such as *Cymothoa* sp., *Nerocila* sp. and *Anilocra* sp. (Bullar 1876), in which the gonad consists of three testis lobes associated with the ovarian lobe that continues as the vas deferens and laterally as the oviduct towards the respective genital aperture. The testes of terrestrial, free living, non-hermaphroditic isopods (*Oniscus asellus*, *Porcellio scaber*), marine free living non-hermaphroditic isopods (*Saduria entomon*) and free living, protandrous hermaphroditic isopods (*Rhyscotus* sp.) are unusually long and slender (Nichols 1902; Jackson 1928; Becker and Mann 1938; Hryniewiecka-Szyfter and Tyczewska 1992). The testis of *N. indica*, however, comprises of three bulged sac-like lobes whose neck opens to the antero-lateral side of the ovary. The histological and ultrasections have muscle layers in the testis wall; when they contract, the spermatophores get released into the ovary, similar to the inference made in *O. asellus* (Nichols 1902).

According to Bullar (1876), the generative organs in cymothoids resemble the combined male and female organs of free living isopods and the parasitic forms probably evolved from their free-living counterparts. The vas deferens in *P. scaber* is divided into anterior and posterior region, which are separated by a constriction; but in hermaphroditic species, the anterior region of the vas deferens represents the ovary (Becker and Mann 1938). In *N. indica*'s M1, the ovary acts as a passage for the spermatophore to move from the testis lobes into the vas deferens. This study agrees with the views of previous investigators (Bullar 1876; Becker and Mann 1938) because it found that the ovary of *N. indica* could be regarded as the anterior vas deferens described in free living forms. Wagele (1992) stated this portion as the seminal vesicle where the spermatophores accumulate. But the present study shows that in *N. indica* the ovary functions in both male and female phases and undergoes drastic microscopic changes right from the M2 size class.

The results of the morphological, histological and ultrastructural observations indicate that oocytes as well as follicle cells are kept active throughout the ovary in the male phase. Apart from morphological variations, the follicle cells display vesicles, mitochondria, ER, free ribosomes and basophilic and electron-dense heterochromatin-containing nuclei, which reflect their secretory function, likely keeping the spermatophores viable while they are in the ovary and before they enter the vas deferens. The oocyte*s* also appear exceptional in that their distinctly large nucleus along with mitochondria, RER and many large multi vesicular bodies signify their secretory nature right from M2. However, histological and histochemical studies also depict the presence of secretory oocytes, and their role, if any, in maintaining the spermatophores is a prime subject for further investigation. The oocytes in M2 are not encircled by follicle cells, but in M3 the typical oocyte with multiple nuclei are found enveloped by the follicle cells.

The giant cells in the anterior expanded portion of vas deferens of *O. asellus* and *P. scaber* were shown to be secretary, and their role in spermatophore sheath formation has been suggested (Nichols 1902; Newsted and Dornfeld 1965). Histologically, the vas deferens of *N. indica* throughout the male phase displays has a glandular cell lining, and its lumen contents has shown high positivity to protein and carbohydrate tests. The viability of spermatophores in the vas deferens is apparently maintained by the secretions of these glandular cells.

Though the testes in juvenile *N. indica* have homogenous cells, in prestaged M1 (post moulted juvenile) and other male size classes (M1, M2 and M3), histology shows that the cells are actually diverse, with somatic accessory cells and germ cells undergoing spermatogenesis and spermiogenesis. In the testis lobes, remarkable regionalization makes the germ cells distinct, which is akin to the report in *S. entomon* (Hryniewiecka-Szyfter and Tyczewska 1992). In *S. entomon*, while the spermatogonia occupy only a narrow bottom portion of each testis tubule, the primary spermatocytes fill all parts of its lumen (Hryniewiecka-Szyfter and Tyczewska 1992). In the M3 class of *N. indica*, the spermatogonia and spermatocytes are seen at one half of the testis lobe, where the spermatogonia are few in number and found in the periphery. Close to the spermatocytes in the centre are the spermatids, and next to those are spermatids undergoing advanced stage of spermiogenesis; adjacent to these spermatids are spermatophores. However, this pattern of arrangement is not uniform in M1, M2 and M3 and germ cell development is not synchronous in testis lobes (t_1, t_2 and t_3). For instance, in M2, t_1 hasspermatogonia and spermatocytes undergoing meiotic division, but no spermatids or spermatophores, while t_2 has spermatocytes and spermatids and t_3 has spermatocytes, spermatids and spermatophores. This asynchrony in germ cell development in the three testis tubules has also been reported in *O. asellus* (Nichols 1902) and *S. entomon* (Hryniewiecka-Szyfter and Tyczewska 1992). In *S. entomon*, the first testis tubule is occupied by secondary spermatocytes and young spermatids and the second and third by maturing spermatids and

spermatozoa, respectively. Though rare, the testes in *N. indica* showed vacant spaces in the testis lobe, likely due to the release of spermatophores.

The aggregation of maturing spermatids and spermatophores close to the *N. indica*'s somatic accessory cells indicates that these cells are significant for spermatophore formation. Ultrastructural investigations of *O. asellus* and *A. vulgare* suggest that accessory cells play a role in forming extracellular tubules surrounding the spermatozoa in the spermatophores (Reger and Fain-Maurel 1973; Itaya 1979). Hryniewiecka-Szyfter et al. (1999) reported that the arrangement of the spermatids around the accessory cells determines the structure of the spermatophore. According to Gabala (2008), accessory cells in *S. entomon* are involved in protein synthesis and formation of the spermatid sheath.

The process in *N. indica* of transforming spermatid to spermatozoon is similar to that reported in *O. asellus* (Nichols 1902) and *S. entomon* (Gabala 2008). The nucleus of the spermatid bulges out at one side to form the acrosomal vesicle, while the heterochromatin condenses and adheres closely to the nuclear envelope to form incomplete rings of variable thicknesses, depending on its distribution towards both the periphery and the nuclear pole. The nuclear pole gradually elongates and ultimately transforms into a ribbon-like structure by simultaneously reducing the cytoplasm and degenerating the vesicular part of the nucleus. A study on spermiogenesis in *S. entomon* (Gabala 2008) describes the changes in the appearance of golgi bodies, accumulation of mitochondria and ribosomes in the cytoplasmic pole of the spermatid associated with the formation of the acrosome vesicle.

The appearance of aflagellate, immotile spermatozoon in *N. indica* is common in the terrestrial free-living and non-hermaphroditic isopod species (Fain-Maurel et al. 1975; Cotelli et al. 1976; Reger et al. 1979; Trovato et al. 2011). But spermatozoon in *N. indica* are shorter (0.38 mm) than in other investigated isopods; for instance, in *P. scaber*, the reported length is 0.8 mm (Cotelli et al. 1976). The presence of an exceptionally long non-motile tail in the isopod sperm deviates from the normal flagellar sperm in the animal kingdom (Pochon-Masson 1978). According to Morrow (2004), aflagellate sperm production is less costly, in terms of energy and time, than the production of motile sperm. However, the loss of sperm motility raises the question of how fertilization occurs in isopods (Wilson 1991 for a review). In *P. scaber*, the two mitochondrial-rich sphincter muscles in the lower vas deferens of the male push spermatophores along the intromittent organ into the female (Radu and Craciun 1972). The histochemical tests being for positive for polysaccharides and proteins in the tail of *N. indica* support the observation and suggestion of Reger (1964) that the tail's rigid structure helps orient the sperm, if it is propelled along the female tract by extrinsic factors. Trovato et al. (2011) confirmed the presence of a large amount of F-actin in the amorphous part of the acrosome and thus suggested that the isopod sperm acquires temporary motility at some point over the course of its interaction with the female gamete. Further investigation of the egg's surface organization and morphological/molecular aspects of gamete interaction could resolve this question of how fertilization occurs in isopods.

The extracellular tubules associated with the spermatophores of *N. indica* are restricted to the acrosome and nucleus and do not extend to the tail. Since the spermatophores in the ovary and vas deferens are found in such a way that their head orients downward, the possible role of these tubules may be to maintain the orientation of spermatophores. Cotelli et al. (1976) and Itaya (1979) has explained the role of extracellular tubules in maintaining the shape of the elongated nuclei and arrangement of individual sperm in the spermatophore in the free-living non-hermaphroditic isopod.

It is well established that the androgenic gland controls the differentiation of the primary and secondary sexual characteristics in crustaceans (Cerveau et al. 2014). The sequence of changes in the primary and secondary sexual characters during sex reversal from male to female in *Irona far* is reported to be associated with the degeneration of the androgenic gland. The androgenic gland was found to masculinize both primary and secondary sexual characteristics in the land isopod, *Armadillidium vulgare* (Legrand 1955; Katakura 1961) through implantation experiments. In *S. entomon*, a set of cells was reported that resembles the androgenic gland in *P. scaber* (Hryniewiecka-Szyfter and Tyczewska 1992). In *N. indica*, the androgenic gland appears to be the most prominent structure in all the male size classes (M1, M2 and M3); the question of the involvement of this gland in protandrous hermaphroditic reproduction in parasitic isopods needs to be addressed in the research ahead.

In addressing the question of how protandrous hermaphroditism in *N. indica* and other cymothoids can be advantageous, it is obvious that protandrous hermaphroditic sex change leads to the formation of large females and hence increased in reproductive potential (Ghiselin 1969; Warner 1975 1988). But male mating success remains independent of size (Shuster and Wade 1991a). For instance, the males in *Paracereis sculpta*, a marine isopod, occurs as three distinct morphotypes representing alternative reproductive

strategies (Shuster 1987), but the average mating success among individuals is statistically equivalent (Shuster and Wade 1991a b). Future research should focus on this aspect of parasitic isopods.

CONCLUSIONS

The present study aimed to understand protandric hermaphroditic changes in the reproductive system of the male-phased cymothoid and the findings will pave way for future in-depth studies on physiological, endocrinological and molecular mechanisms. This, in turn, would be useful to predict the significance of protandric hermaphroditism adopted by cymothoids, if any, for their obligatory parasitic life on host fishes and such information may help formulate strategies for cymothoid management in the aquaculture sector.

Acknowledgments: SK gratefully acknowledges the Kerala State Council for Science, Technology and Environment, Government of Kerala (No. (T) 093/ SRS/2011/CSTE; Dated: 25/06/2011), Department of Science and Technology, Govt. of India DST-SERB (EMR/2016/001163 dated 28.08.2017) and Kerala State Council for Science, Technology and Environment, Government of Kerala (No. 02/DIR/2017-18/KSCSTE dated, 03/04/2018) for helping to financially support this work and prepare the manuscript. We thank Prof. G Anilkumar for his help reviewing and editing the manuscript.

Authors' contributions: HA worked on the topic as the project fellow under a research project funded by the Kerala State Council for Science, Technology and Environment, Government of Kerala (No. (T) 093/ SRS/2011/CSTE; Dated: 25/06/2011) and wrote the first draft of the manuscript. SK, the aforesaid project's Principal Investigator and HA's PhD Mentor, drew out the concept, supervised the work, interpreted the results and finalized the manuscript. All authors read and approved the final manuscript.

Competing interests: The authors declare that they have no conflict of interests.

Availability of data and materials: All data and materials for this project can be found in the article.

Consent for publication: Consent is given.

Ethics approval consent to participate: This article does not contain any studies with human participants or animals performed by any of the authors.

REFERENCES

Allen JA. 1959. On the biology of *Pandalus borealis* Kroyer, with reference to a population off the Northumberland coast. J Mar Biol Assoc UK **38(1):**189–220.

Aneesh PT. 2014. Studies on parasitic crustaceans infesting the fishes of Malabar Coast (PhD dissertation). Kannur University, Kerala.

Aneesh PT, Helna AK, Sudha K. 2015a. Branchial Cymothoids infesting the marine food fishes of Malabar Coast. J Parasit Dis **40(4):**1270–1277. doi:10.1007/s12639-015-0666-0.

Aneesh PT, Sudha K, Arshad K, Anilkumar G, Trilles JP. 2013. Seasonal fluctuation of the prevalence of cymothoids representing the genus *Nerocila* (Crustacea, Isopoda), parasitizing commercially exploited marine fishes from the Malabar Coast, India. Acta Parasitol **58:**80–90. doi:10.2478/ s11686-013-0112-3.

Aneesh PT, Sudha K, Helna AK, Anilkumar G, Trilles JP. 2014. Multiple parasitic crustacean infestation on belonid fish *Strongylura strongylura*. ZooKeys **457:**339–353. doi:10.3897/ zookeys.457.6817.

Aneesh PT, Sudha K, Helna AK, Anilkumar G, Trilles JP. 2015b. *Cymothoa frontalis*, a cymothoid isopod parasitizing the belonid fish, *Strongylura strongylura* from the Malabar coast (Kerala, India): redescription, prevalence and life cycle. Zool Stud **54:**42. doi:10.1186/s40555-015-0118-7.

Aneesh PT, Sudha K, Helna AK, Anilkumar G. 2018. *Agarna malayi* Tiwari 1952 (Crustacea: Isopoda: Cymothoidae) parasitising the marine fish, *Tenualosa toli* (Clupeidae) from India: re-description/description of parasite life cycle and patterns of occurrence. Zool Stud **57:**25. doi:10.6620/ZS.2018.57-25.

Bauer RT, Holt GJ. 1998. Simultaneous hermaphroditism in the marine shrimp *Lysmata wurdemanni* (Caridea: Hippolytidae): an undescribed sexual system in the decapod Crustacea. Mar Biol **132(2):**223–235.

Becker FD, Mann ME. 1938. The reproductive system of the male isopod, *Porcellio scaber* Latreille. Trans Am Microsc Soc **57(4):**395–399.

Brook HJ, Rawlings TA, Davies RW. 1994. Protogynous sex change in the intertidal isopod *Gnorimosphaeroma oregonense* (Crustacea: Isopoda). Biol Bull **187(1):**99–111.

Buchanan JB. 1963. The biology of *Calocarismacandreae* (Crustacea: Thalassinidea). J Mar Biol Assoc UK **43(03):**729–747.

Bullar JF. 1876. The generative organs of the parasitic Isopoda. J Anat Physiol **11:**118-123.

Cerveau N, Bouchon D, Bergès T, Grève P. 2014. Molecular evolution of the androgenic hormone in terrestrial isopods. Gene **540(1):**71–77. doi:10.1016/j.gene.2014.02.024.

Cook CW. 2012. The early life history and reproductive biology of *Cymothoa excisa*, a marine isopod parasitizing Atlantic croaker, (*Micropogonias undulatus*), along the Texas coast. PhD dissertation, University of Texas.

Cotelli F, Ferraguti M, Lanzavecchia G, Donin CL. 1976. The spermatozoon of Peracarida. I. The spermatozoon of terrestrial isopods. J Ultrastruct Res **55(3):**378–390.

Cressey RF. 1983. Crustaceans as parasites of other organisms. Biol Crustacea **6:**251–273.

Elshahawy IS, Desouky AY. 2012. First record of *Mothocya melanosticta* Schioedte and Meinert, 1884 (Isopoda: Cymothoidae) from Egyptian pinecone soldier fish with special reference to its infestation status. Turk J Vet Anim Sci **36(6):**577–584.

Fain-Maurel MA, Reger JF, Cassier P. 1975. Le gamete mâle des schizopodesetses analogies avec celui des autrespéracarides: I. Le spermatozoïde. J Ultrastruct Res **51(2):**269–280.

Gabala E. 2008. Ultrastructure of spermiogenesis in the marine isopod *Saduriaentomon* (Crustacea, Isopoda). Invertebr Reprod Dev **51(1):**33–47. doi:10.1016/j.asd.2007.11.004.

Ghiselin MT. 1969. The evolution of hermaphroditism among animals. Q Rev Biol **44(2):**189–208.

Hadfield KA, Bruce NL, Smit NJ. 2013. Review of the fish-parasitic genus *Cymothoa Fabricius*, 1793 (Isopoda, Cymothoidae, Crustacea), from the southwestern Indian Ocean, including a new species from South Africa. Zootaxa **3640(2):**152–176.

Helna AK. 2016. Studies on growth and reproduction of parasitic crustaceans infesting scombrid fishes along the Malabar Coast. PhD dissertation, Kannur University, Kerala, India.

Hryniewiecka-Szyfter Z, Tyczewska J. 1991. The histology of the male reproductive system of *Saduriaentomon* (Linnaeus, 1758) (Isopoda, Valvifera). Crustaceana **60(3):**246–257.

Hryniewiecka-Szyfter Z, Tyczewska J. 1992. Morphological organization of the female reproductive system of *Saduriaentomon* (Linnaeus, 1758) (Isopoda, Valvifera). Crustaceana **63(1):**1–10.

Hryniewiecka-Szyfter Z, Gabala E, Babula A. 1999. The role of sertoli cells in the organization of sperm bundles in the testis of *Saduriaentomon* (Linnaeus, 1758) (Isopoda, Valvifera). Crustaceana **72(9):**1067–1078.

Humason GL. 1967. Animal tissue techniques. Fourth edition. W.H. Freeman and Company, San Franscisco.

Itaya PW. 1979. Electron microscopic investigation of the formation of spermatophores of *Armadillidium vulgare*. Cell Tissue Res **196(1):**95–102.

Jackson HG. 1928. Hermaphroditism in *Rhyscotus*, a terrestrial isopod. Q J Microsc Sci **71:**527–539.

Juchault P. 1965. Contribution à l'étude de la différenciation sexuelle mâle chez les Crustacés Isopodes (Doctoral dissertation, SFIL et imp. Marc Texierréunies.

Katakura Y. 1961. Hormonal control of development of sexual characters in the isopod crustacean, *Armadillidium vulgare*. Annotationes zoologicae Japonenses **34:**197–199.

Legrand JJ. 1952. Contribution à l'étude expérimentale et statistique de la biologie d'*Anilocra physodes* L. (Crustacé Isopode Cymothoidé). Archs Zool exp gén **89(1):**1–56.

Legrand JJ. 1955. Rôleendocrinien de lovairedans la différenciation des oostégites chez les Crustacés Isopode sterrestres. Comptes rendus hebdomadaires des Séances de l'Academie des Sciences **241(16):**1083–1085.

Morrow EH. 2004. How the sperm lost its tail: the evolution of aflagellate sperm. Biological Reviews **79(04):**795–814.

Newstead JD, Dornfeld EJ. 1965. Epithelial structure in the anterior segment of the vas deferens of an isopod, *Porcellio scaber* (Latreille). Z Zellforsch Mik Ana **68:**795–817.

Nichols ML. 1902. The Spermatogenesis of *Oniscus asellus* Linn., with especial reference to the history of the chromatin. Proc Am Philos Soc **41:**77–112.

Pearse AGE. 1968. Histochemistry: theoretical and applied, 3rd. ed., Vol. I. Little, Brown and Co., Boston, 759 pp.

Pochon-Masson J. 1978. Les différenciations infrastructurales liées a la perte de la motilité chez les gametes mâles des Crustacés. Archs Zool exp gén **119:**465–470.

Radu VG, Craciun C. 1972. Ultrastructure du segment terminal du canal déférent chez Porcellio scaber Latr. Rev Roum Biol, Ser Zool **17:**167–173.

Reger JF. 1964. The fine structure of spermatozoa from the isopod *Asellus militaris* (Hay). J Ultrastruct Res **11(1):**181–192.

Reger JF, Fain-Maurel MA. 1973. A comparative study on the origin, distribution, and fine structure of extracellular tubules in the male reproductive system of species of isopods, amphipods, schizopods, copepods, and cumacea. J Ultrastruct Res **44(3):**235–252.

Reger JF, Itaya PW, Fitzgerald ME. 1979. A thin section and freeze-fracture study on membrane specializations in spermatozoa of the isopod, *Armadillidium vulgare*. J Ultrastruct Res **67(2):**180–193.

Schram F, von Vaupel Klein C, Charmantier-Daures M, Forest J. (Eds.) 2012. Treatise on Zoology-Anatomy, Taxonomy, Biology. The Crustacea, Volume 9 Part B: Eucarida: Decapoda: Astacidea P.P. (Enopometoploidea, Nephropidea) Glypheidea, Axiidea, Gebiidea, and Anomura (partim) (Vol. 9).

Shuster SM. 1987. Alternative reproductive behaviors: Three discrete male morphs in paracerceis sculpta, an intertidal isopod from the northern gulf of california. J Crust Biol **7:**318–327.

Shuster SM, Wade MJ. 1991a. Equal mating success among male reproductive strategies in a marine isopod. Nature **350:**608.

Shuster SM, Wade MJ. 1991b. Female copying and sexual selection in a marine isopod crustacean, paracerceis sculpta. Anim Behav **41:**1071–1078.

Subramoniam T. 2013. Origin and occurrence of sexual and mating systems in Crustacea: A progression towards communal living and eusociality. J Biosci **38(5):**951–969.

Subramoniam T. 2016. Sexual Biology and Reproduction in Crustaceans. Academic Press, Elsevier.

Trilles JP, Ravichandran S, Rameshkumar G. 2011. A checklist of the cymothoidae (Crustacea, Isopoda) recorded from Indian fishes. Acta Parasitol **56(4):**445–459. doi:10.1007/s00436-012-3263-5.

Trovato M, Mazzei V, Sinatra F, Longo G. 2011. Presence of F-actin in sperm head of *Armadillidium peraccae* (Isopoda, Oniscidea). Tissue Cell **43(5):**304–310. doi:10.1016/j.tice.2011.06.002.

Tsai ML, Li JJ, Dai CF. 1999. Why selection favors protandrous sex change for the parasitic isopod, *Ichthyoxenus fushanensis* (Isopoda: Cymothoidae). Evol Ecol **13(4):**327–338.

Wagele JW. 1992. Isopoda: Harrison F.W. & Humes A.G. (eds): Microscopic anatomy of Invertebrates 9; Crustacea, pp. 529–611.

Warner RR. 1975. The adaptive significance of sequential hermaphroditism in animals. Am Nat **109:**61–82.

Warner RR. 1988. Sex change in fishes: hypotheses, evidence, and objections. Environ Biol Fishes **22(2):**81–90.

Wilson GDF. 1991. Functional morphology and evolution of isopod genitalia. *In*: Bauer RT, Martin JW (ed.), Crus sex biol, Columbia University Press, New York.

Williams DB, Carter CB. 1996. Transmission electron microscopy: A textbook for materials science. New York: Plenum Press.